

2 **Solar Irradiance Modulation of Equator-to-Pole (Arctic) Temperature Gradients:**  
3 **Empirical Evidence for Climate Variation on Multi-decadal Timescales**

4  
5 **Willie Soon**<sup>1</sup> (wsoon@cfa.harvard.edu) and **David R. Legates**<sup>2</sup> (legates@udel.edu)

6 <sup>1</sup>Harvard-Smithsonian Center for Astrophysics, Cambridge MA 02138, USA

7 <sup>2</sup>College of Earth, Ocean, and Environment, University of Delaware, Newark, DE 19716, USA

8  
9 **Abstract**

10 Using thermometer air temperature records for the period 1850 to 2010, we present empirical  
11 evidence for a direct relationship between total solar irradiance (TSI) and the Equator-to-Pole  
12 (Arctic) surface temperature gradient (EPTG). Modulation of the EPTG by TSI is also shown to  
13 exist, in variable ways, for each of the four seasons. Interpretation of the positive relationship  
14 between the TSI and EPTG indices suggests that solar-forced changes in the EPTG may  
15 represent a hemispheric-scale relaxation response of the system to a reduced Equator-to-Pole  
16 temperature gradient, which occurs in response to an increasing gradient of incoming solar  
17 insolation. Physical bases for the TSI-EPTG relationship are discussed with respect to their  
18 connections with large-scale climate dynamics, especially a critical relationship with the total  
19 meridional poleward energy transport. Overall, evidence suggests that a net increase in the TSI,  
20 or in the projected solar insolation gradient which reflects any net increase in solar radiation, has  
21 caused an increase in both oceanic and atmospheric heat transport to the Arctic in the warm  
22 period since the 1970s, resulting in a reduced temperature gradient between the Equator and the  
23 Arctic. We suggest that this new interpretative framework, which involves the extrinsic  
24 modulation of the total meridional energy flux beyond the implicit assumptions of the Bjerknes  
25 Compensation rule, may lead to a better understanding of how global and regional climate has  
26 varied through the Holocene and even the Quaternary (the most recent 2.6 million years of  
27 Earth's history). Similarly, a reassessment is now required of the underlying mechanisms that  
28 may have governed the equable climate dynamics of the Eocene (35 to 55 million years ago) and  
29 late Cretaceous (65 to 100 million years ago), both of which were warm geological epochs. This  
30 newly discovered relationship between TSI and the EPTG represents the "missing link" that was  
31 implicit in the empirical relationship that Soon (2009) recently demonstrated to exist between  
32 multi-decadal TSI and Arctic and North Atlantic climatic change.

## 33 1. Introduction

34  
35 A study of Sun-climate relationships is, in the strictest sense, a search for self-consistent dynamic  
36 evidence that connects variable solar magnetic activity with robust measures of regional- and  
37 hemispheric-scale climate and other relevant variables including surface and atmospheric  
38 temperature and precipitation (see Weng 2005; Soon 2009; Gray *et al.* 2011; Soon *et al.* 2011;  
39 and Weng 2012a,b for a broad overview and relevant references). To understand large-scale  
40 ocean-atmosphere circulation dynamics and their impact on climate, many authors stress the  
41 importance of Equator-to-Pole temperature gradients and heat fluxes as fundamental and robust  
42 expressions of the Earth's coupled land-ocean-atmosphere climate system (*e.g.*, Stone 1978;  
43 Farrell 1990; Lindzen 1994; Jain *et al.* 1999; Pierrehumbert 2002; Enderton and Marshall 2009;  
44 Vallis and Farneti 2009; Lee *et al.* 2011; Huang *et al.* 2012; Karamperidou *et al.* 2012; Rose and  
45 Ferreira 2012; Weng 2012a). Building on this research, our study provides empirical evidence  
46 for a physical relationship between varying Total Solar Irradiance (TSI) and the Northern  
47 Hemispheric Equator-to-Pole Temperature Gradient (EPTG), based on instrumental data records  
48 and extrapolative analyses. This new empirical evidence may constitute the “missing link”  
49 suggested by earlier research that showed an empirical link between TSI and Arctic and North  
50 Atlantic climatic changes (Soon 2009).

51  
52 It is our thesis that the observed relationship between TSI and EPTG represents the large-scale  
53 thermal and dynamic relaxation response of the coupled ocean-atmosphere climate system to the  
54 externally imposed multi-decadal variation in solar irradiance. Although known changes in TSI  
55 are not exceptionally large (on the order of a few tenths of a percent of the TSI over the last 400  
56 years), they are sufficient to constitute an actual change in the total radiant energy added or  
57 subtracted to the climate system. Rather than being a mere redistribution of shortwave radiation  
58 energy, as in the case of Sun-Earth orbital changes that have been well-studied for the warm  
59 interglacials and ice ages of the Quaternary (Laskar *et al.* 1993, Laskar *et al.* 2011), the  
60 possibility exists for a direct increase or decrease in the total poleward energy transport. This  
61 implies that both the oceanic and atmospheric heat transport can simultaneously increase or  
62 decrease as a result of variations in TSI.

63  
64 Latitudinal insolation gradients are the key drivers and/or modulators of the differential  
65 latitudinal temperature gradients. Moreover, the varying latitudinal distribution of insolation in  
66 response to orbital changes at Milankovitch frequencies also played a dominant role in  
67 controlling climate change during the Holocene and the glacial-interglacial changes of the  
68 Quaternary (Raymo and Nisancioglu 2003; Kukla and Gavin 2005; Liu *et al.* 2008; Davis and  
69 Brewer 2009).

70  
71 Our hypothesis is testable by measurement and compilation of the key physical signatures of  
72 ocean and atmosphere heat transport. These empirical data can then be compared with the  
73 implicit assumptions of the Bjerknes compensation, which assumes the maintenance of a  
74 constant total poleward energy transport that then provides an internally self-regulating inverse  
75 relation between oceanic and atmospheric heat transport fluxes (Bjerknes 1964; Shaffrey and  
76 Sutton 2006; Enderton and Marshall 2009; Rose and Ferreira 2012; Zelinka and Hartmann 2012).  
77 We discuss the available empirical evidence from actual oceanographic observations and  
78 assimilated atmospheric and oceanic circulation, and thermal conditions from climate models,

79 which together suggest the possibility that a simultaneous increase in poleward oceanic and  
80 atmospheric heat transport did in fact occur during the most recent warming period since the  
81 mid-1970s.

82  
83 From theoretical formulations, Stone (1978) isolated the ‘solar constant’ as one of the most  
84 important drivers of the total meridional heat transport, and also one that is largely independent  
85 of the dynamical adjustment processes internal to the Earth climate system. Enderton and  
86 Marshall (2009), however, cautioned that Stone (1978)’s general conclusion should be modified  
87 to incorporate changes in the meridional gradients of albedo under the scenario of cold climate  
88 regimes that are associated with significant changes in polar ice cap size and sea-ice cover.  
89 Donohoe and Battisti (2012) estimated that for the current climate, the direct meridional  
90 distribution of incident radiation contributed about 65% of the absorbed solar radiation, while the  
91 35% contribution from net planetary albedo is apportioned to be 30% by atmospheric reflection  
92 and only 5% by surface reflection. Using numerical models in relation to the effects of ocean  
93 geometry, Vallis and Farneti (2009) have attempted an even more general exploration of the  
94 properties of meridional energy transport oceanic diapycnal diffusivity, moisture content of the  
95 atmosphere, distribution of solar radiation, and the rotation rate of the Earth. Importantly, Vallis  
96 and Farneti (2009) concluded that there is no *á priori* constraint on the total meridional heat  
97 transport in the coupled ocean-atmosphere system of the Earth. In other words, to gain a more  
98 complete and correct interpretation of the available instrumental and proxy records of climatic  
99 variations, it may be necessary to relax the assumption of the Bjerknes compensation for  
100 poleward atmospheric and oceanic heat transport.

101  
102 In this regard, our discussion sheds light on similar queries raised in the recent review by  
103 Wunsch (2010: 1965): “What [is] surprising is that one rarely if ever sees the question raised as  
104 to how the global heat budget is then maintained [if the meridional oceanic heat transport is  
105 diminished]? Does the atmosphere respond by increasing its transport – getting warmer and/or  
106 wetter – as in Bjerknes (1964) compensation?” These are important fundamental questions that  
107 we seek to answer.

108  
109 Turning to hydrological effects of changing TSI, Agnihotri *et al.* (2011) proposed the time  
110 derivative of TSI as a relevant metric for studying hydrologic changes and variations. Kukla and  
111 Gavin (2005) argued for the importance of the intensification of the hydrologic cycle, both  
112 through an increased meridional insolation gradient and through warming of tropical oceans and  
113 cooling of the Polar Regions. They argued that these processes control the inception of major  
114 glaciation in Northern Hemisphere land areas, including the Last Glacial Maximum. Such a  
115 physical boundary condition (*i.e.*, the persistent increase in the meridional insolation gradient as  
116 a result of a specific Sun-Earth orbital configuration) for high northern latitude glaciations can be  
117 expected for Sun-Earth orbital configuration of low obliquity coinciding with perihelion in  
118 Northern Hemisphere winters. Davis and Brewer (2011) proposed a new framework to  
119 encompass all sources of changes in the latitudinal insolation gradient, noting that orbital, solar-,  
120 and lunar-induced forcings are all strongly connected to the atmospheric and oceanic circulation  
121 of the Earth system. Our study supplements this important discussion by identifying a more  
122 realistic physical constraint on TSI. In this context, the framework of Davis and Brewer could  
123 add a fresh insight to the underlying mechanisms and feedbacks governing the Equable climate

124 dynamics<sup>1</sup> of the Eocene (35 to 55 million years ago) and late Cretaceous (65 to 100 million  
125 years ago) warm epochs (*e.g.*, Sluijs *et al.* 2006; Greenwood *et al.* 2010; Eberle and Greenwood  
126 2012; Kroeger and Funnell 2012; Pross *et al.* 2012). Observations suggest that the direct  
127 modulation of the total ocean-atmospheric meridional heat transport by changes in TSI is rooted  
128 in the intrinsic variability of the Sun’s magnetic activity. Therefore, our proposed mechanism  
129 provides an efficient and realistic way to warm the high-latitude polar regions and mid-latitudes  
130 that does not create concomitantly large temperature changes in the tropics. To explain the Early  
131 Eocene warming, for example, Huber and Caballero (2011) were forced to postulate perhaps  
132 unrealistic atmospheric CO<sub>2</sub> levels of 2240 or even 4480 ppm for the Early Eocene (see Hong  
133 and Lee 2012 on the paleo-CO<sub>2</sub> constraints of no more than 1500 ppm) that warmed not only the  
134 Arctic and Antarctic regions but also the tropics significantly (up to 40-50°C were simulated in  
135 the tropics). We may add that with the new palynological evidence that confirms mild winter  
136 temperatures greater than 10°C at Wilkes Land coast, Antarctica during the early Eocene epoch  
137 (Pross *et al.* 2012), our hypothesis of an efficient TSI-induced modulation and control of the  
138 equator-to-pole heat transports should be seriously considered.

139

## 140 **2. TSI and Northern Hemisphere EPTG Data: Sources and Physical Motivations**

141

142 The solar radiation parameter adopted here is based on the comprehensive reconstruction of total  
143 solar irradiance (TSI) by Hoyt and Schatten (1993), which derives from multiple solar activity  
144 proxies (see discussion below). Scafetta and Willson (2009; 2012, private communication) have  
145 updated and re-scaled this TSI series through 2010. Note that since 1979, satellite-based cavity  
146 radiometers have measured the absolute level of TSI to lie between 1360 and 1375 Wm<sup>-2</sup>, while  
147 physical modeling yields a theoretical value of 1379.9 Wm<sup>-2</sup> (Fontenla *et al.* 2011). We have  
148 used the newer value of TSI obtained by ACRIM-3 (Active Cavity Radiometer Irradiance  
149 Monitor-3) which indicates that from 1979 to 2011, TSI ranged between 1360 and 1363 Wm<sup>-2</sup>  
150 (Willson 2011). This value is consistent with the suggested calibrated values of about 1361 Wm<sup>-2</sup>  
151 by the PREMOS (Precision Monitoring Sensor onboard the PICARD satellite mission)  
152 experiments (W. Schmutz 2012, private communication<sup>2</sup>) and also with the value of 1360.8 ± 0.5  
153 Wm<sup>-2</sup> estimated by Kopp and Lean’s (2011) Total Irradiance Monitor (TIM). Based on their  
154 comprehensive nature, we believe the estimates from Hoyt and Schatten/Scafetta and Willson to  
155 be the most reliable estimates of TSI currently available (see further discussion below).

156

157 The impact of uncertainties in the absolute value of TSI on globally-averaged surface air  
158 temperature, or on the derived EPTG, is not discussed in detail here. Nevertheless, an  
159 acknowledgement of the uncertainty in TSI is a prerequisite for the proper assessment of the  
160 dynamic evolution of the weather-climate system. In addition, knowledge regarding the long-  
161 term variation in solar spectral irradiance (*e.g.*, see discussion of the impacts of solar UV  
162 variations on the response of the coupled stratosphere-troposphere chemistry and dynamics in

---

<sup>1</sup> Farrell (1990) pointed out that the thin Earth’s atmosphere is remarkably effective in transferring heat between the equator and pole. Without the poleward dynamic heat flux and heat flux divergence, the equator-to-pole temperature gradient is estimated to be 109°C with a very warm equator of 50°C. Farrell notes that because of the short (less than monthly) time scale of radiative forcing in a non-rotating atmosphere, EPTG should be even much smaller than what is observed today. Thus, the puzzle for the Earth’s climate system is indeed “not that equable climates occur, it is that they are not the norm.” (p. 2987)

<sup>2</sup> Werner Schmutz is PI of PREMOS/PICARD; this also was noted on page 5 of the PMOD/WRC 2010 Annual Report.

163 Soon 2009; Gray *et al.* 2011; Hood and Soukharev 2012), such as reported by Fontela *et al.*  
164 (2011), must be incorporated into future studies to progress our understanding of sun-climate  
165 relationships.

166  
167 Before 1979, TSI was reconstructed using proxies for solar magnetic activity and its variability,  
168 including empirical results from long-term monitoring of Sun-like stars (Baliunas *et al.* 1995;  
169 Lockwood *et al.* 2007; Hall *et al.* 2009). Our reason for choosing the TSI reconstruction from  
170 Hoyt and Schatten (1993) is mainly because their work involves the most diverse types and  
171 ranges of proxy values for solar irradiance estimation – sunspot cycle amplitude, sunspot cycle  
172 length, solar equatorial rotation rate, fraction of penumbral spots, and the decay rate of the  
173 approximate 11-year sunspot cycle. Their assumption was that each of these slightly different  
174 proxies will most likely capture some part of the underlying factors responsible for modulating  
175 the solar magneto-convection-induced processes that affect TSI. In an *á priori* sense, we note  
176 that all these magneto-fluid dynamical processes on the Sun need not strictly follow an 11-year-  
177 like cycles of high-and-near-zero in sunspot numbers as that specified artificially by the  
178 paleoclimate modeling community (see Figure 5 of Schmidt *et al.* 2011). We judge that this  
179 multi-proxy approach to TSI reconstruction is more likely to be consistent with the physical  
180 modeling of solar irradiance outputs of Fontenla *et al.* (2011), who adopted as many as nine solar  
181 features<sup>3</sup> describing the range of magnetic fields in the networks and active regions. Moreover,  
182 the TSI reconstruction by Hoyt and Schatten (1993) may facilitate a more self-consistent study of  
183 the multi-decadal modulation of the EPTG because the solar equatorial rotation rate exhibits  
184 considerable change in the early 20th century (see Figure 1 of Hoyt and Schatten 1993).

185  
186 Moreover, the TSI reconstruction of Hoyt and Schatten (1993) using multiple solar-variability  
187 proxies is more consistent with the work of Fontenla *et al.* (2011) than other TSI reconstructions,  
188 which are often based on a model with sunspot blocking and faculae brightening, or alternatively,  
189 are based solely on geomagnetic activity indices. Evidence suggests that even the “quiet” part of  
190 the Sun may simply consist of small-scale magnetic fields that vary in both mean strength and  
191 spatial distribution which in turn may or may not relate to the dark magnetic spot activity  
192 variations (Caccin *et al.* 1998; Schuhle *et al.* 2000; Trujillo Bueno *et al.* 2004; Orozco Suarez *et*  
193 *al.* 2007; Kleint *et al.* 2010; Schnerr and Spruit 2011; Orozco Suarez and Rubio 2012; Stenflo  
194 2012; Stenflo and Kosovichev 2012).

195  
196 It is relevant to note that in Shapiro *et al.* (2011), the amplitude of the total solar irradiance  
197 change between the Maunder Minimum and current conditions was determined to be  $6 \pm 3 \text{ Wm}^{-2}$   
198 – a value significantly larger than estimates by some other authors but in good agreement with  
199 the estimate of Zhang *et al.* (1994), based on their study of the Sun and other Sun-like stars. The  
200 results of Shapiro *et al.* (2011) are consistent with the amplitude of total solar irradiance used  
201 here that was deduced independently by Hoyt and Schatten (1993). Another recent paper by  
202 Judge *et al.* (2012), however, argued that the TSI estimates by Shapiro *et al.* (2011) may have  
203 been overestimated by a factor of two which further adds to the uncertainty to the correct  
204 estimate for the amplitude of TSI variations over the past 400 years.

205

---

<sup>3</sup> These features are (1) Dark quiet-Sun inter-network, (2) Quiet-Sun inter-network, (3) Quiet-Sun network lane, (4) Enhanced network, (5) Plage (that is not facula), (6) Facula (i.e., very bright plage), (7) Sunspot umbra, (8) Sunspot penumbra and (9) Hot facula.

206 Instead of using mean global air temperature, as is the usual choice, our primary motivation for  
 207 considering the EPTG is that EPTG constitutes a more fundamental description/expression of the  
 208 global climate system and of climate dynamics in general (see Lindzen 1994; Karamperidou *et al.*  
 209 2012; Weng 2012a). Lindzen (1994) interpreted the global mean surface temperature to be  
 210 simply a residual product of the change in the Equator-to-Pole temperature distribution while,  
 211 importantly, the EPTG contains more useful information on climate dynamics than does the  
 212 global mean air temperature. The new theoretical analyses by Rose and Ferreira (2012) tend to  
 213 support this interpretation. Furthermore, Karamperidou *et al.* (2012:4156) highlighted the fact  
 214 that “the magnitude of the post-1976 trend of [EPTG] is not as striking as the one of the global  
 215 mean temperature anomalies during the same period ... rather, it is comparable to [the EPTG] of  
 216 the 1870-1940 period.” A recent study of sea-level pressure and sea surface temperature by van  
 217 Loon *et al.* (2012) identifies a relatively steeper pressure and temperature gradient between the  
 218 Arctic and lower latitude regions of the Atlantic during the 1878-1944 interval compared to the  
 219 much weaker or reduced gradient at the 1944-2008 period. van Loon *et al.* (2012) interpreted  
 220 this result to indicate the clear dependence of the surface pressure and temperature gradients (and  
 221 hence the strength and intensity of the quasi-stationary wave and baroclinic eddies in the North  
 222 Atlantic region) on the phases of the 80-100 years Gleissberg solar activity cycles.

223  
 224 We also note that the derived EPTG may offer a superior interpretation and attribution of the  
 225 processes responsible for the changes in global air temperature that have been observed since  
 226 1976. The EPTG probably is the best available index/proxy for the 1979-1998 warming,  
 227 especially when one considers the great complexity and difficulty involved in removing potential  
 228 non-climatic or socio-economical influences from the surface thermometer data records (*e.g.*,  
 229 McKittrick and Michaels 2007; Fall *et al.* 2011; McKittrick and Tole 2012).

### 230 231 **3. Calculation of the EPTG**

232  
 233 To calculate the EPTG indices, we have modified the method used by Jain *et al.* (1999) and  
 234 Karamperidou *et al.* (2012) by deleting the areal weighting. Our rationale is that we are  
 235 interested in the gradient that exists in the meridional direction only. Thus, each latitudinal band  
 236 is averaged in the zonal direction and the EPTG is calculated as the slope of these zonal averages.  
 237 Mathematically, this is equivalent to an unweighted regression slope,

$$238 \quad \text{EPTG} = \frac{\sum_{i=1}^n (T_i - \bar{T})(\theta_i - \bar{\theta})}{\sum_{i=1}^n (\theta_i - \bar{\theta})^2} \quad (1)$$

239  
 240  
 241 where  $\theta_i$  is the latitude and  $T_i$  is the temperature of the  $i^{\text{th}}$  zonally-averaged grid box ( $n$  total  
 242 boxes) and the overbar indicates a hemispheric/latitudinal band average. The summation holds  
 243 over all the 72x18 longitude-latitude boxes available from the gridded 5°x5° surface air  
 244 temperature database of the University of East Anglia. By including latitudinal weights to  
 245 account for areal averaging, as applied by Jain *et al.* (1999), the tropics are given undue and  
 246 unwarranted influence (*i.e.*, one half of the Northern Hemisphere lies between 0° and 30°N)  
 247 which obscures the true meridional gradient. Again, we stress that we are interested in  
 248 computing the Equator-to-Pole temperature *gradient*, which is independent of the decreasing  
 249 area toward the Pole. Thus, the areal weighting used by Jain *et al.* (1999) and Karamperidou *et*  
 250 *al.* (2012) is not appropriate for our analysis and has been removed.

251  
252 Other formulations of the EPTG exist (see Figure 5 of Davis and Brewer 2011). Gitelman *et al.*  
253 (1997) defined their ‘meridional temperature gradient’ as the difference in temperature between  
254 the 30° to 35° latitudinal band and the 50° to 55° latitudinal band, later changing this to range  
255 between the 0° to 25° latitudinal band and the 65° to 90° latitudinal band (Rind 1998; Gitelman  
256 *et al.* 1999). Braganza *et al.* (2003) defined the EPTG as the temperature difference between the  
257 22.5° to 37.5° latitudinal band and the 52.5° to 67.5° latitudinal band. We argue that the  
258 calculation of a hemispheric slope is preferable to the rather arbitrary selection of latitudinal  
259 bands for, as Gitelman *et al.* (1999:16709) noted, the EPTG “is sensitive to the choice of  
260 latitudes used to define it” with “substantial differences in behavior on timescales from  
261 interannual to multidecadal.” These points also are well-taken by Jain *et al.* (1999), who note  
262 that observational data are sparse poleward of about 70°N and equatorward of about 15°N, which  
263 adversely affects the calculation of the gradient. To remedy this, we have further examined the  
264 gradient from 0° to 30°N, 30°N to 60°N, and 60°N to 90°N, in addition to the entire hemisphere,  
265 to identify relative contributions and to examine data inconsistencies in these regions. Note too  
266 that these other formulations of the EPTG are consistent with our modification of Jain *et al.*  
267 (1999) to remove the adjustment for the decreasing area toward the Pole.

268  
269 An arguably better measure of the EPTG – calculation of the temperature difference between the  
270 tropical surface and the polar upper-troposphere/tropopause – was proposed by Lindzen (2012).  
271 Lindzen’s argument is that this metric better measures the meridional transport of heat along  
272 isentropic surfaces (see Figure 10 of his paper) as poleward transport of energy occurs through  
273 baroclinic eddies. We will examine this measure and its relationship to TSI in a subsequent  
274 paper.

275  
276 Monthly, seasonal, and annual mean values of the EPTG were calculated using the gridded 1850-  
277 to-2010 instrumental surface temperature record available from the University of East Anglia’s  
278 Climatic Research Unit (HadCRUT3 – Brohan *et al.* 2006; Rayner *et al.* 2006; downloaded  
279 August 16, 2009). We place less emphasis on the early part of the record (prior to 1920) due to  
280 the sparseness of the data; most notably, poor spatial sampling in the Arctic region. It is worth  
281 noting that other researchers have also limited their analysis to exclude the early years –  
282 Gitelman *et al.* (1999) started after 1854, while Gitelman *et al.* (1997), Rind (1998), and  
283 Braganza *et al.* (2003) began in 1880 and Jain *et al.* (1999) began in 1898. Though other  
284 observational databases could have been used, Gitelman *et al.* (1999) achieved nearly identical  
285 results using both HadCRUT3 data and the GISS dataset (Hansen and Lebedeff 1987). Details  
286 of our computation of EPTG metric, and the sensitivity and comparison of the metric with other  
287 data records (*i.e.*, the 20<sup>th</sup> century reanalysis of Compo *et al.*, 2011, and the University of  
288 Alabama-Huntsville MSU lower troposphere temperature dataset) will be reported in a separate  
289 paper.

290  
291 To emphasize multi-decadal variation, a ten-year running mean filter was applied to the raw  
292 EPTG series only (but not to the TSI series). We further note that our main focus is to study  
293 physical relationships between solar irradiance and climate dynamics on multidecadal timescales  
294 and a ten-year running mean filter specifically avoids effects related to short-term weather  
295 variability. Soon (2009) and Soon *et al.* (2011) provide additional physical arguments for  
296 separation of the multidecadal-to-centennial scale variability from weather variability. Note that

297 the TSI series is not smoothed as there is a strong eleven-year solar cycle that might be aliased  
298 into lower frequency signals if it were smoothed. Ultimately, the distinction between the so-  
299 called “top-down” solar forcing-climatic response scenario from the “bottom-up” scenario will  
300 be likely important and useful. This is because the “bottom-up” solar-climatic connection  
301 pathway may operate more efficiently and dominantly in the multidecadal to centennial  
302 timescales while the “top-down” scenario will more obviously manifest under the powerful  
303 control of the 11-year solar irradiance contrasts between the 11-year solar activity maxima and  
304 minima (see Hood and Soukharev 2012; van Loon and Meehl 2012 and references therein).

305  
306 It is important to note that since the HadCRUT3 data are anomalies from a standard period, our  
307 values of the EPTG are anomalies from the average Equator-to-Pole temperature gradient, which  
308 is strongly negative (*i.e.*, the Pole is colder than the Equator) and on the order of  $-0.5^{\circ}\text{C}/\text{degree}$   
309 latitude. Positive values therefore indicate gradients which are less negative (warmer Pole and/or  
310 colder Equator) while negative values indicate an enhanced EPTG (warmer Equator and/or  
311 colder Pole).

312  
313 Correlation can be problematic when temporal autocorrelation is high, as is often the case with  
314 many environmental variables (*e.g.*, Yue *et al.* 2002; Hamid 2009; 2011). Yue *et al.* (2002) and  
315 Hamid (2009; 2011) argue that non-parametric correlation coefficients such as Spearman’s Rho  
316 (Spearman 1904) or Kendall’s Tau (Kendall 1938) are preferable to the often-used Pearson’s  
317 Product-Moment Correlation Coefficient. We agree with such concerns and, to remedy this  
318 potential problem, we have employed both the Coefficient of Determination (*i.e.*, the square of  
319 the Pearson Product-Moment Correlation Coefficient) and Kendall’s Tau to judge the magnitude  
320 of the statistical correlation. In addition, we have limited the correlation analysis to the period  
321 from 1880 to 2010 to reduce the impact of the early, data-sparse years (*i.e.*, 1850 to 1879).

322  
323 Due to serial autocorrelation in the data, assessment of statistical significance must include its  
324 effect on the coefficients. Here, we use an ‘effective sample size’ to accommodate temporal  
325 autocorrelation by augmenting the ‘effective degrees of freedom’ (see Laurmann and Gates  
326 1977; Thiebaut and Zwiers 1984). Rather than simply using the total number of years minus  
327 one as the degrees of freedom, autocorrelations determined that independence occurred at a lag  
328 of fourteen years. This reduced our ‘effective sample size’ to ten rather than the 131 years of the  
329 record (*i.e.*, 1880 to 2010). Thus, the ‘effective degrees of freedom’ that we used to assess  
330 statistical significance reflects this smaller sample size.

#### 331 332 **4. Results and discussion**

333  
334 The relationship between the TSI and the annual-mean Northern Hemisphere EPTG over the  
335 instrumental surface air temperature period from 1850 to 2010 (Figure 1) shows that variation in  
336 TSI can explain 36% of the yearly mean EPTG with a Kendall’s Tau of 0.43. The explained  
337 variance increases to 70% and Kendall’s Tau increases to 0.63 when a ten-year running mean is  
338 applied to smooth the EPTG (which accentuates multi-decadal-scale variation; see Table 1).  
339 Soon (2009) and Soon *et al.* (2011) have previously shown that variability at multi-decadal  
340 timescales on the order of 40 to 80 years is prominent in most solar and climatic records.

341

342 Figure 2 offers evidence that the multi-decadal variation in the Northern Hemisphere EPTG is  
343 more prominently expressed in the 60°N to 90°N zonal band, with most of the variability in the  
344 Northern Hemisphere EPTG being caused by the variability in the polar region (*i.e.*, 89% of the  
345 variance explained in the ten-year smoothed time-series). This strong latitudinal dependence of  
346 the TSI-EPTG relation is expected owing to relatively faster thermal responses at the 60-90°N  
347 bands than the mid-latitude (30°N to 60°N) and tropical (0° to 30°N) bands. The statistical  
348 analyses reported in Table 1, however, suggest that the correlations between TSI and latitudinal  
349 surface temperature gradients computed over the midlatitude bands (30°N to 60°N), especially  
350 for the spring season, are also statistically robust and hence physically plausible. We note that  
351 the lack of statistical correlation between the EPTG and TSI within the tropical band (0° to  
352 30°N) does not contradict our hypothesis. Consequently, we examine a possible connection  
353 between the Northern Hemisphere EPTG and the strength of the northern component of the  
354 tropical Hadley circulation as deduced by Liu *et al.* (2012) below.  
355

356 When grouped into winter (DJF), spring (MAM), summer (JJA), and autumn (SON), the  
357 relationship between TSI and the EPTG shows that despite large interannual variability, multi-  
358 decadal-scale oscillations are quite prominent in the winter and spring and, more surprisingly, in  
359 summer as well (Figure 3). About 60% of the variation in the ten-year smoothed EPTG for  
360 these three seasons can be explained by the TSI and the value of Kendall's Tau lies between 0.51  
361 and 0.58 (Table 1). Variability at the 40- to 80-year time-scale is well-represented during the  
362 summer despite high solar incidence angles over the Northern Hemisphere which should produce  
363 weaker temperature contrasts between the tropics and the high Arctic.  
364

365 The Coefficients of Determination (*i.e.*,  $r^2$ ) between TSI and the seasonal air temperature  
366 gradients between the Equator and the Arctic are consistent with the results of Soon (2005) and  
367 other seasonal energy budget studies of Arctic surface temperatures (*e.g.*, Semmler *et al.* 2005).  
368 Moreover, additional multi-decadal climate signatures have been discovered in the Arctic and  
369 nearby impacted and remotely teleconnected regions (see Soon 2009; Soon *et al.* 2011). Soon *et al.*  
370 (2011) found an unexpected multi-decadal summer climate connection with TSI over East  
371 Asia that they interpreted as forced by the circum-global teleconnection pattern of summer  
372 circulation (Ding and Wang 2005). We wish to add that the emphasis on summer season-  
373 associated climate dynamics may have empirical supports from paleoclimate proxy data where  
374 relative variations in summer temperature on multidecadal to centennial timescales are often  
375 found to be larger than those during winter season (see *e.g.*, Jiang *et al.* 2005; Kamenos 2010).  
376 Cohen *et al.* (2012) described a recent phase of boreal winter cooling between 1988 and 2010  
377 that was likely preconditioned and forced by warming tendencies in the preceding summer and  
378 autumn seasons. Alexeev *et al.* (2012) noted that the persistent 1960s to 1980s Arctic cooling  
379 tendency in the upper troposphere and lower stratosphere switched to a warming tendency  
380 around 1990 (see Figure 7 in their paper). The authors suggest that this switch is consistent with  
381 the well-known multi-decadal variations in near-surface-subsurface climatic and oceanographic  
382 conditions that dominate the Arctic and North Atlantic. An exciting challenge for the future is to  
383 establish a sound model for the physical processes that underlie the observed empirical  
384 correlations between TSI and EPTG.  
385

386 We argue that the strength and physical consistency of the observed sun-climate relationship  
387 suggests strongly that a causal link exists. We have provided evidence that the association

388 between TSI and EPTG may be more than just a random chance occurrence. Thus, the following  
389 interpretations are proposed and a possible testable consequence of putative physical  
390 relationships is suggested.

391  
392 We contend that the observed relationship between TSI and EPTG in this paper is based upon the  
393 latter representing the large-scale thermal and dynamical relaxation response of the coupled  
394 ocean-atmosphere climate system to incoming solar irradiance. Soon *et al.* (2011) posited  
395 evidence of just such a Sun-climate link operating in the East Asian monsoonal region. The  
396 empirical evidence shown in Soon *et al.* (2011) supports the idea that multi-decadal variation of  
397 incoming solar radiation is not limited solely to TSI (or the top-of-the-atmosphere solar  
398 insolation). Rather, the intensity of solar radiation reaching the surface has a persistent multi-  
399 decadal oscillatory character that depends on the nature of changing atmospheric transmissivity,  
400 including the effects of clouds, pollution, aerosols, *etc.*

401  
402 Our premise, therefore, is that as TSI increases, the projected insolation gradient between the  
403 tropic and Arctic regions increases proportionately, thereby leading to an increase in the  
404 poleward atmospheric and/or oceanic heat transport<sup>4</sup> which decreases the surface temperature  
405 gradients between the Equator and the Arctic (*i.e.*, towards more positive values of the EPTG  
406 index shown in Figures 1, 2 and 3). In contrast, the poleward heat transport decreases when  
407 TSI decreases thus causing an increase in the Equator-to-Arctic temperature gradient<sup>5</sup> (*i.e.*,  
408 towards more negative values of the EPTG index). Although multi-decadal scale changes in TSI  
409 are only on the order of a few tenths of a percent (see summary discussion in Section 2), these  
410 changes represent an actual increase/decrease in the total radiative energy being added  
411 to/subtracted from the climate system, not simply a mere redistribution of solar energy (*i.e.*, with  
412 no large net change in incoming solar radiant energy) as occurs through Sun-Earth orbital  
413 changes at 19-to-23 kyr, 41 kyr to 100 kyr time-scales (*i.e.*, Milankovitch variables). This  
414 suggests a physical basis for a direct increase or decrease in the total poleward energy transport  
415 as a result of direct variations in the incoming solar radiation. We add that our postulated  
416 mechanism may be able to provide the necessary increase (rather than decrease) in “energy” or  
417 “heat” that is needed for the production of glacial epochs, as originally proposed by Tyndall  
418 (1872) and Croll (1890)<sup>6</sup> and as more recently highlighted in Kukla and Gavin (2005), who  
419 focused solely on orbital-induced modulation of the incoming insolation.

---

<sup>4</sup> In this, our initial study and analysis, the specific effects from local and regional insolation gradients that may potentially drive and/or modulate specific atmospheric and oceanic circulation phenomena will not be discussed. For example, Lindzen and Pan (1994) pointed out the mechanism in which orbital control on the off-equator maximum heating in the summer hemisphere can lead to strong modulation of the Hadley circulation intensity and hence lead to a significant modulation of the equator-to-pole heat fluxes in the opposing winter hemisphere. Please also see also the new discussion paper by Liu et al. (2012) where the evidence for the variations in the strength and width of the Hadley Circulation on multidecadal to centennial scales is given.

<sup>5</sup> Here, we argue that TSI drives the insolation gradient and the EPTG is the relaxation response.

<sup>6</sup> From Kukla and Gavin (2004:28), we find that Tyndall (1872:154) noted that “So natural was the association of ice and cold that even celebrated men assumed that all that is needed to produce a great extension of our glaciers is a diminution of the sun’s temperature. Had they gone through the foregoing reflections and calculations, they would probably have demanded *more* [sic.] heat instead of less for the production of a ‘glacial epoch’.” From Kukla and Gavin (2005:1555), we find that Croll (1890) noted that “A general reduction of temperature over the whole globe certainly would not produce a glacial epoch. Suppose the sun were extinguished and our globe exposed to the temperature of the stellar space; this would certainly freeze the ocean solid from its surface to its bottom, but it would not cover the land with ice.”

420

421 This testable hypothesis is considered to be the key physical relationship that underlies our  
422 proposed Sun-climate connection. Available empirical evidence supports an increase in both  
423 oceanic and atmospheric poleward heat transport, especially in the recent warming since the  
424 1980s. Thus, the goal is to reconcile these facts with the implicit assumptions of the Bjerknes  
425 compensation, which assumes maintenance of a *constant* total poleward energy transport  
426 controlled by an internally self-regulating inverse relation between oceanic and atmospheric heat  
427 transport fluxes (see Bjerknes 1964; Shaffrey and Sutton 2006; Enderton and Marshall 2009;  
428 Rose and Ferreira 2012; Zelinka and Hartmann 2012). In this regard, the observations of Czaja  
429 and Marshall (2006:1509) are very encouraging: “Our results suggest that the oceanic and  
430 atmospheric heat transport might themselves change rather modestly in very different climate  
431 states. In other words, climate variability may be associated with only small departures from a  
432 fixed background [atmospheric and oceanic heat transport] curves.”

433

434 Vallis and Farneti (2009) have noted correctly that no *á priori* reason exists to suppose that the  
435 total poleward heat transport must have remained constant throughout any period of Earth’s  
436 history. Nonetheless, surprisingly few attempts have been made to estimate the total meridional  
437 heat transport of the Earth’s climate system over any time scale, though over short recent periods  
438 some authors have partitioned heat flow into its atmospheric and oceanic components, from both  
439 *in situ* and/or satellite observations (see Trenberth and Caron 2001; Wunsch 2005). Wunsch  
440 (2005) noted that the calculation of the total meridional heat transport by Trenberth and Caron  
441 (2001) is ultimately based on constraints set by the Earth Radiation Budget Experiment (ERBE),  
442 data that cover only three years of observations (1987 to 1989).<sup>7</sup> Despite this limitation, the  
443 available data indicate that the maximum atmospheric heat transport lies between  $3 \times 10^{15}$  and  
444  $5 \times 10^{15}$  W at around 36°N, while the oceanic heat transport reaches a comparable figure  
445 between 0° to about 28°N with a maximum of  $2 \times 10^{15}$  W at low latitudes (Wunsch 2005).  
446 Considering a maximum total meridional heat transport of  $6 \times 10^{15}$  W at around 40°N and with  
447 surface area poleward of 40°N of about  $5.6 \times 10^{13}$  m<sup>2</sup> (*i.e.*, about 100 Wm<sup>-2</sup>), the incoming solar  
448 radiation of about 340 W/m<sup>2</sup> (*i.e.*, the solar constant divided by 4) is more than sufficient to  
449 account for the poleward energy transport budget. This calculation suggests that there is no need  
450 to invoke any energy “amplification” to explain solar climate forcing – as is often required and  
451 discussed within a so-called “radiative forcing-feedback” framework – concerning how the solar  
452 TSI or radiation can affect or modulate weather-climate changes on Earth.

453

454 Huang (2005:279) cautioned against assuming that the oceanic transport component is not  
455 important beyond the tropics just because much of the atmospheric transport is in the form of  
456 latent heat and because the ocean provides atmospheric water vapor that is circulated poleward<sup>8</sup>:  
457 “Thus, the heat transport process starts from the ocean, and it ends in the atmosphere, so the

---

<sup>7</sup> We note that the ERBE radiation budget data studied by Trenberth and Caron (2001) covers the interval from February 1985 to April 1989.

<sup>8</sup> The interpretive framework suggested by Huang (2005) in separating the poleward heat flux into three components – (1) atmospheric sensible heat flux, (2) oceanic sensible heat flux and (3) atmosphere-ocean-land coupled latent heat flux – is likely more physically reasonable. Huang (2005) summarized that “in both hemispheres, poleward heat flux is carried by three components that work like a relay team. In the subtropics the oceanic sensible heat flux is the dominating contributor to the poleward heat flux divergence, and in mid-latitudes the latent heat flux divergence is the dominating contributor. Finally, in high latitudes the atmospheric sensible heat flux divergence dominates.”

458 latent heat flux loop is really a coupled mode.” The new analyses of Rose and Ferreira (2012)  
459 support this “relay-transport” picture of Huang (2005) in that “the climatic impact of OHT  
460 [Ocean Heat Transport] depends on its effect on the greenhouse properties of the atmosphere [*i.e.*,  
461 through enhanced deep moist convection within midlatitude storm tracks], rather than its ability  
462 to increase the total poleward energy transport” (Rose and Ferreira, 2012:1). Huang (2005) also  
463 clarified that it is not the heat flux *per se* that is important for the discussion on climate and  
464 climate variability; but rather, the divergence of those heat fluxes on local and regional scales.  
465 Pierrehumbert (2002) noted that despite the expected large increase in dry static energy transport  
466 resulting from the high Equator-to-Pole temperature gradient during the Last Glacial Maximum,  
467 the significant drop in the latent heat transport associated with the cooler subtropics led to very  
468 little overall increase in the poleward heat flux transported from the tropics, as is indeed reflected  
469 in some computer climate simulations (*e.g.*, Murakami *et al.* 2008).

470  
471 What evidence is available to show how the atmospheric and oceanic meridional heat fluxes  
472 transport energy poleward? Detailed discussion of that question is limited because it is nearly  
473 impossible to accurately partition the differing sources of the heat transport associated with, *inter*  
474 *alia*, the Hadley circulation, atmospheric eddies or various oceanic surface currents, and  
475 subsurface meridional overturning circulation. As a first step towards that end, we are  
476 nonetheless encouraged by the plausible relationship that existed between the total Northern  
477 Hemisphere EPTG index and the northern component of the strength of the Hadley circulation  
478 (as deduced by Liu *et al.* 2012) from 1871 to 2008.

479  
480 Observational, model-derived, and theoretical/numerical analyses can also shed light on the  
481 increased atmospheric poleward heat transport that must have been associated with the Arctic  
482 warming during the last quarter of the 20<sup>th</sup> century. Using the available observational and  
483 assimilated data records, the analyses of Graversen *et al.* (2008), Smedsrud *et al.* (2008), Zhang  
484 *et al.* (2008), Yang *et al.* (2010), Screen and Simmonds (2010), and Alexeev *et al.* (2012)<sup>9</sup>,  
485 despite some disagreements in the details,<sup>10</sup> all point to a net increase in the atmospheric heat  
486 flux to the Arctic since 1979. For example, Smedsrud *et al.* (2008 – see their Figure 1a) and  
487 Yang *et al.* (2010 – see their Figure 1) confirm increases in atmospheric heat transport to the  
488 Arctic and in its decadal variation, respectively. Alexeev *et al.* (2012) have documented a more  
489 coherent and consistent warming in the lower stratosphere (200 to 70 mb), especially above the  
490 Canadian Arctic, as compared to variations in the lower and middle troposphere. They argued  
491 that the warming of the lower stratosphere, and the inferred overall weakening of polar vortex, is  
492 consistent with the coherent multi-decadal variability found for the Arctic and North Atlantic  
493 near-surface climate and oceanic variables on timescales of 50 to 80 years. Theoretical studies  
494 using mainly climate models of various complexity (Caballero and Langen 2005; Langen and  
495 Alexeev 2007; Hwang and Frierson 2010; Cvijanovic *et al.* 2011; Wu *et al.* 2011; Zelinka and

---

<sup>9</sup> We caution that the claim by Alexeev *et al.* (2012:217) that “Graversen *et al.* (2008) found such an elevated warming in the winter and summer temperature trends, which they argued was not strongly linked to poleward atmospheric heat transport” is opposite to what Graversen *et al.* (2008) actually concluded in their paper. Instead, Graversen *et al.* (2008:53) said that “We concluded that changes in atmospheric heat transport may be an important cause of the recent Arctic temperature amplification”.

<sup>10</sup> For example, both Screen and Simmond (2011) and Alexeev *et al.* (2012) note that an instrumental artifact arises from the switch between two different satellite radiance databases during 1997 in the 40-year European Centre for Medium-Range Weather Forecasts Re-Analysis product. This disjunction adversely affects the reliability of atmospheric temperature profiles for the Arctic region that use this product.

496 Hartmann 2012) also confirm an increased poleward atmospheric energy transport resulting from  
497 a generic global-scale warming<sup>11</sup>. Although they focused only on interannual variability, Huang  
498 *et al.* (2012) also examine this issue, and suggest that the ocean exhibits a ‘memory’ for  
499 transferring both the atmospheric angular momentum and its total energy between tropics and  
500 polar regions.

501  
502 The existence of increased oceanic heat transport into the Nordic Seas and its subsequent entry  
503 into the Arctic Basin has been confirmed by both oceanographic observations and data-  
504 assimilated modeling efforts (*e.g.*, Orvik and Skagseth 2005; Polyakov *et al.* 2005; Hansen *et al.*  
505 2008; Holliday *et al.* 2008; Sarafanov *et al.* 2008; Hakkinen and Rhines 2009; Jackson *et al.*  
506 2010; Polyakov *et al.* 2010a; 2010b; Toole *et al.* 2010; Willis 2010; Robson *et al.* 2012).  
507 Hakkinen and Rhines (2009) discuss the observational evidence from 1990 to 2007 that shows an  
508 increased penetration of warm and saline subtropical waters toward the Nordic Seas which, in  
509 turn, is noted as the key region that supports the Atlantic Meridional Overturning Circulation  
510 (MOC), involving the creation, sinking and southward-flow of water at intermediate and deeper  
511 depths. The Atlantic MOC is the main modulator of how heat and salt (freshwater) are  
512 transported into and from the northern North Atlantic Ocean and the Arctic Basin (see Latif *et al.*  
513 2004; 2006). Citing the observational results of Belkin *et al.* (1998), Hakkinen and Rhines  
514 (2009) added that the observed oceanographic conditions and poleward penetration of the  
515 subtropical warm and saline waters in the northern North Atlantic Ocean for the 1990s and mid-  
516 2000s were perhaps not a unique phenomenon. As they state, “A longer time series exists from  
517 the Faroe-Shetland Channel which shows that even higher upper ocean salinities were  
518 encountered in the 1930s until about 1940...when a major warming occurred in the Atlantic  
519 subpolar zone” (Hakkinen and Rhines 2009:10). The climate modeling study of Robson *et al.*  
520 (2012) suggests further that the rapid warming of the North Atlantic Ocean in the mid-1990s was  
521 primarily a result of “a surge in the northward ocean heat transport”. In addition, Polyakov *et al.*  
522 (2005; 2010a; 2010b) have tracked how the Arctic Basin was warmed by the penetration of  
523 warm and saline Atlantic waters of intermediate depths (150 to 900 meters) through the 1990s,  
524 culminating with the intense warming and heating of the Arctic Ocean from below that occurred  
525 in 2007.

526  
527 Similarly, much research has focused on the Pacific component of Arctic water as well.  
528 Shimada *et al.* (2006) documented a positive, atmospheric circulation-sea ice, motion feedback-  
529 induced influx of warm Pacific water that occurs in summer at relatively shallower (50 to 100  
530 meters) depths and within less saline (as compared to the Atlantic intermediate-depth waters)  
531 waters that flow through Bering Strait and into the Canadian Basin of the Arctic. It is this influx  
532 of warm Pacific water that caused the sea surface warming and maximum melting of sea ice  
533 there around 1998-2003. Woodgate *et al.* (2010) estimated that heat fluxes carried by the influx  
534 of Pacific waters through the Bering Strait increased from about 2 to 3 x 10<sup>20</sup> J yr<sup>-1</sup> in 2001 to a  
535 maximum of 5 to 6 X 10<sup>20</sup> J yr<sup>-1</sup> in 2007. They suggest that the amount of heat flux was  
536 “somewhat greater than the incoming shortwave solar [radiation] input into the Chukchi Sea”  
537 and would have been enough to account for one-third of the 2007 Arctic sea ice loss (Woodgate  
538 *et al.* 2010:5). Bourgain and Gascard (2012: 1) offer another independent data analysis when  
539 they conclude:

---

<sup>11</sup> Here, only research resulting from analyses without any direct radiative forcing from increasing CO<sub>2</sub> concentrations has been cited to avoid impacts arising from changes in atmospheric constituents.

540  
541 “Observations confirmed the existence of warm pulses of the Atlantic water mass  
542 propagating into the Arctic basin. However, no warming trend of the Atlantic  
543 water in the Eurasian basin was identified over the 1997-2008 time period. In  
544 contrast, the Summer Pacific water was getting warmer ... [and] appears to be a  
545 serious candidate for contributing partly to the drastic summer sea ice extent and  
546 thickness decrease observed recently in the Arctic and in the Canadian basin in  
547 particular.”

548  
549 Clearly, Bourgain and Gascard (2012) disagree with Polyakov *et al.* (2010a). But it is important  
550 to note that Polyakov *et al.* (2010a) place strong emphasis on the importance of the role of multi-  
551 decadal variability within the North Atlantic and Arctic. In this sense, their conclusion is fully  
552 consistent with the multi-decadal variations in both surface temperature and salinity of the North  
553 Atlantic subpolar gyre that were shown by Reverdin (2010).

554  
555 Despite the patchy nature of these adventitious, historical oceanographic data records, these  
556 results are consistent with a simultaneous increase in both atmospheric and ocean meridional  
557 heat transport in the Arctic Basin during the late 20<sup>th</sup> century. Such a fact, which has yet to be  
558 fully confirmed, would indicate violation of the Bjerknes compensation rules (see Czaja and  
559 Marshall 2006; Shaffrey and Sutton 2006; Enderton and Marshall 2009; Vallis and Farneti 2009;  
560 Zelinka and Hartmann 2012 for additional insights).

561  
562 Further evidence concerning how the Equator-to-Pole heat and moisture fluxes change on multi-  
563 decadal to centennial timescales arises from a study by Lund *et al.* (2006). These authors found  
564 that the Florida Current, and by inference the Gulf Stream, probably flowed at a substantially  
565 reduced rate of about  $3\pm 1$  Sv during the Little Ice Age (about 1200 to 1850 A.D.). This would  
566 be consistent with a reduced poleward heat and moisture transport during a relatively cold period  
567 of reduced TSI. Such an empirical deduction is not inconsistent with the qualitative scenarios  
568 sketched by Mörner (2010) concerning the multidecadal-to-centennial-scale modulation of the  
569 flow dynamics of the Gulf Stream, including even the increasing southward penetration of cold  
570 Arctic-originated water, during cold intervals of the Little Ice Age owing to the mass, energy and  
571 angular momentum readjustments from the increasing Earth rotation rate. However, the caution  
572 posited by Huybers and Wunsch (2010:1) is clearly valid; namely, that “few features of the  
573 paleo-circulation in any period are yet known with certainty.”

## 574 575 **5. Conclusion**

576  
577 We assert that strong evidence exists to support the reality of a physical Sun-climate connection,  
578 as manifest in the multi-decadal co-variations of TSI and EPTG. A similar relationship also  
579 exists between fluctuations in TSI and other regional-scale climate variables such as surface air  
580 temperature. Our study clearly implies a necessity to account for the persistent nature of this  
581 external solar irradiance forcing. Many previous studies have amply documented relevant  
582 physical relationships, which range across seasonal, decadal, multi-decadal, centennial and  
583 millennial timescales. The empirical relationships regarding modern climate that are shown in  
584 this paper have great potential for application to the interpretation of climate variability in other  
585 geological epochs, before the modern era of instrumental and satellite-borne measurements. We

586 suggest that fruitful exploration of the topic might first be made using records from the data-rich  
587 Holocene epoch.

588 **Acknowledgements**

589

590 We thank Dr. Nicola Scafetta for sharing with us the updated and re-scaled TSI series based on  
591 Hoyt and Schatten (1993) proxy series and ACRIM satellite radiometers results. We also wish to  
592 thank Drs. Gene Avrett, Steve Cranmer, Juan Fontenla, Demetris Koutsoyiannis, Richard  
593 Lindzen, Niklas Mörner, Harry van Loon and three anonymous referees, for their careful reading  
594 of the manuscript and constructive criticisms, comments and improvements. We also thank Dr.  
595 Gil Compo for helpful answers on the 20<sup>th</sup> Century Reanalysis dataset and Drs. Jiping Liu and  
596 YongYun Hu for their generosity in sharing some of their new results and data series on Hadley  
597 circulation. Willie Soon would also like to extend his appreciation to Julia Pham, Benjamin and  
598 Franklin Soon, David and Steve Fettig, Sallie Baliunas, Bob Carter, Juan Ramirez, Dennis  
599 Mitchell and Geoff Smith for encouraging him to continue his scientific research in  
600 understanding the Sun-climate connection.

601 **References**

- 602 Agnihotri, R., Dutta, K., and Soon, W. (2011) Temporal derivative of Total Solar Irradiance and  
603 anomalous Indian Summer monsoon: An empirical evidence for a sun-climate connection.  
604 *Journal of Atmospheric and Solar-Terrestrial Physics*, vol. 73, 1980-1987.  
605
- 606 Alexeev, V.A., Esau, I., Polyakov, I.V., Byam, S.J., and Sorokina, S. (2012) Vertical structure of  
607 recent Arctic warming from observed data and reanalysis products. *Climatic Change*, vol. 111,  
608 215-239.  
609
- 610 Baliunas, S.L., and 26 co-authors (1995) Chromospheric variations in main-sequence stars. II.  
611 *The Astrophysical Journal*, vol. 438, 269–287.  
612
- 613 Belkin, I.M., Levitus, S., Antonov, J., and Malmberg, S.-A. (1998) “Great Salinity Anomalies”  
614 in the North Atlantic. *Progress in Oceanography*, vol. 41, 1-68. [See also Corrigendum in  
615 *Progress in Oceanography*, vol. 45, 107-108, (2000)]  
616
- 617 Bjerknes, J. (1964) Atlantic air-sea interaction. *Advances in Geophysics*, vol. 10, 1-82.  
618
- 619 Bourgain, P., and Gascard, J.-C. (2012) The Atlantic and Summer Pacific waters variability in  
620 the Arctic Ocean from 1997 to 2008. *Geophysical Research Letters*, vol. 39,  
621 doi:10.1029/2012GL051045.  
622
- 623 Braganza, K., Karoly, D.J., Hirst, A.C., Mann, M.E., Stott, P., Stouffer, R.J., and Tett, S.F.B.  
624 (2003) Simple indices of global climate variability and change: Part I – variability and  
625 correlation structure. *Climate Dynamics*, vol. 20, 491-502.  
626
- 627 Brohan, P., Kennedy, J.J., Harris, I., Tett, S.F.B., and Jones, P.D. (2006) Uncertainty estimates  
628 in regional and global observed temperature changes: a new dataset from 1850. *Journal*  
629 *Geophysical Research*, vol. 111, doi:10.1029/2005JD006548.  
630
- 631 Caballero, R., and Langen, P.L. (2005) The dynamic range of poleward energy transport in an  
632 atmospheric general circulation model. *Geophysical Research Letters*, vol. 32,  
633 doi:10.1029/2004GL021581.  
634
- 635 Caccin, B., Ermolli, I., Fofi, M., and Sambuco, A.M. (1998) Variations of the chromospheric  
636 network with solar cycle. *Solar Physics*, vol. 177, 295-303.  
637
- 638 Cohen, J.L., Furtado, J.C., Barlow, M.A., Alexeev, V.A., and Cherry, J.E. (2012) Arctic  
639 warming, increasing snow cover and widespread boreal winter cooling. *Environmental Research*  
640 *Letters*, vol. 7, doi:10.1088/1748-9326/7/1/014007.  
641
- 642 Compo, G.P., and 26 co-authors (2011) The twentieth century reanalysis project. *Quarterly*  
643 *Journal of the Royal Meteorological Society*, vol. 137, 1–28.  
644
- 645 Croll, J. (1890) *Climate and Time* (Edward Stanford, London, 577 pp).  
646

647 Cvijanovic, I., Langen, P.L., and Kaas, E. (2011) Weakened atmospheric energy transport  
648 feedback in cold glacial climates. *Climate of the Past*, vol. 7, 1061-1073.  
649

650 Czaja, A., and Marshall, J. (2006) The partitioning of poleward heat transport between the  
651 atmosphere and ocean. *Journal of the Atmospheric Sciences*, vol. 63, 1498-1511.  
652

653 Davis, B.A.S., and Brewer, S. (2009) Orbital forcing and role of the latitudinal  
654 insolation/temperature gradient. *Climate Dynamics*, vol. 32, 143-165.  
655

656 Davis, B.A.S., and Brewer, S. (2011) A unified approach to orbital, solar, and lunar forcing  
657 based on the Earth's latitudinal insolation/temperature gradient. *Quaternary Science Reviews*, vol.  
658 30, 1861-1874.  
659

660 Ding, Q., and Wang, B. (2005) Circumglobal teleconnection in the Northern Hemisphere  
661 summer. *Journal of Climate*, vol. 18, 3483–3505.  
662

663 Donohue, A., and Battisti, D.S. (2012) What determines meridional heat transport in climate  
664 models? *Journal of Climate*, vol. 25, 3832-3850.  
665

666 Eberle, J.J., and Greenwood (2012) Life at the top of the greenhouse Eocene world—A review of  
667 the Eocene flora and vertebrate fauna from Canada's High Arctic. *Geological Society of America*  
668 *Bulletin*, vol. 124, 3-23.  
669

670 Enderton, D., and Marshall, J. (2009) Explorations of atmosphere-ocean-ice climates on an  
671 aquaplanet and their meridional energy transports. *Journal of the Atmospheric Sciences*, vol. 66,  
672 1593-1611.  
673

674 Fall, S., Watts, A., Nielsen-Gammon, J., Jones, E., Niyogi, D., Christy, J.R., and Pielke Sr., R.A.  
675 (2011) Analysis of the impacts of station exposure on the U.S. Historical Climatology Network  
676 temperatures and temperature trends. *Journal Geophysical Research*, vol. 116,  
677 doi:10.1029/2010JD015146.  
678

679 Farrell, B.F. (1990) Equable climate dynamics. *Journal of the Atmospheric Sciences*, vol. 47,  
680 2986-2995.  
681

682 Fontenla, J.M., Harder, J., Livingston, W., Snow, M., and Woods, T. (2011) High-resolution  
683 solar spectral irradiance from extreme ultraviolet to far infrared. *Journal Geophysical Research*,  
684 vol. 116, doi:10.1029/2011JD016032.  
685

686 Gitelman, A.I., Risbey, J.S., Kass, R.E., and Rosen, R.D. (1997) Trends in the surface meridional  
687 temperature gradient. *Geophysical Research Letters*, vol. 24, 1243-1246.  
688

689 Gitelman, A.I., Risbey, J.S., Kass, R.E., and Rosen, R.D. (1999) Sensitivity of a meridional  
690 temperature gradient index to latitudinal domain. *Journal of Geophysical Research*, vol. 104,  
691 16709-16717.  
692

693 Graversen, R.G., Mauritsen, T., Tjernstrom, M., Kallen, E., and Svensson, G. (2008) Vertical  
694 structure of recent Arctic warming. *Nature*, vol. 451, 53-56. [See Brief Communications Arising  
695 between the authors and Thorne, 2008, Grant et al, 2008, Bitz and Fu, 2008, *Nature*, vol. 455,  
696 E1-E5.]  
697  
698 Gray, L.J., Beer, J., Geller, M., Haigh, J.D., Lockwood, M., Matthes, K., Cubasch, U., Fleitmann,  
699 D., Harrison, G., Hood, L., Luterbacher, J., Meehl, G.A., Shindell, D., van Geel, B., White, W.  
700 (2010) Solar influences on climate. *Reviews of Geophysics*, vol. 48, 1–53.  
701  
702 Greenwood, D.R., Basinger, J.F., and Smith, R.Y. (2010) How wet was the Arctic Eocene rain  
703 forest? Estimates of precipitation from Paleogene Arctic macrofloras. *Geology*, vol. 38, 15-18.  
704  
705 Hakkinen, S., and Rhines, P.B. (2009) Shifting surface currents in the northern North Atlantic  
706 Ocean. *Journal Geophysical Research*, vol. 114, doi:10.1029/2008JC004883.  
707  
708 Hall, J.C., Henry, G.W., Lockwood, G.W., Skiff, B.A., and Saar, S.H. (2009) The activity and  
709 variability of the Sun and sun-like stars. II. Contemporaneous photometry and spectroscopy of  
710 bright solar analogs. *The Astronomical Journal*, vol. 138, 312–322.  
711  
712 Hamed, K.H. (2009) Effect of persistence on the significance of Kendall’s tau as a measure of  
713 correlation between natural time series. *The European Physical Journal – Special Topics*, vol.  
714 174:65-79.  
715  
716 Hamed, K.H. (2011) The distribution of Kendall’s tau for testing the significance of cross-  
717 correlation in persistent data. *Hydrological Sciences Journal*, vol. 56, 841-853.  
718  
719 Hansen, B., Osterhus, S., Turrell, W.R., Jonsson, S., Valdimarsson, H., Hatun, H., and Olsen,  
720 S.M. (2008) The inflow of Atlantic water, heat, and salt to the Nordic Seas across the  
721 Greenland-Scotland ridge. In *Arctic-Subarctic Ocean Fluxes: Defining the Role of the Northern*  
722 *Seas in Climate*, edited by R.R. Dickson, J. Meincke, P.B. Rhines, pp. 15-43, Springer,  
723 Dordrecht, Netherlands.  
724  
725 Hansen, J., and Lebedeff, S. (1987) Global trends of measured surface air temperature. *Journal*  
726 *of Geophysical Research*, vol. 92, 13345-13372, doi:10.1029/JD092iD11p13345.  
727  
728 Holliday, N.P., and 10 co-authors (2008) Reversal of the 1960s to 1990s freshening trend in the  
729 northeast North Atlantic and Nordic Seas. *Geophysical Research Letters*, vol. 35,  
730 doi:10.1029/2008GL032675.  
731  
732 Hong, S.K., and Lee, Y.I. (2012) Evaluation of atmospheric carbon dioxide concentrations  
733 during the Cretaceous. *Earth and Planetary Science Letters*, vol. 327-328, 23-28.  
734  
735 Hood, L.L., and Soukharev, B.E. (2012) The lower stratospheric response to 11-year solar  
736 forcing: Coupling to the troposphere-ocean response. *Journal of the Atmospheric Sciences*, vol.  
737 69, 1841-1864.  
738

739 Hoyt, D.V., Schatten, K.H. (1993) A discussion of plausible solar irradiance variations, 1700-  
740 1992. *Journal of Geophysical Research*, vol. 98, 18895–18906.  
741  
742 Huang, R.X. (2005) Contribution of oceanic circulation to the poleward heat flux. *Journal of*  
743 *Ocean University of China*, vol. 4, 277-287.  
744  
745 Huang, W.-R., Chen, T.-C., and Wang, S.-Y. (2012) Co-variability of poleward propagating  
746 atmospheric energy with tropical and higher-latitude climate oscillations. *Climate Dynamics*, vol.  
747 39, 1905-1912, doi:10.1007/s00382-011-1283-3.  
748  
749 Huber, M., and Caballero, R. (2011) The early Eocene equable climate problem revisited.  
750 *Climate of the Past*, vol. 7, 603-633.  
751  
752 Huybers, P., and Wunsch, C. (2010) Paleophysical oceanography with an emphasis on transport  
753 rates. *Annual Review of Marine Science*, vol. 2, 1-34.  
754  
755 Hwang, Y.-T., and Frierson, D.M.W. (2010) Increasing atmospheric poleward energy transport  
756 with global warming. *Geophysical Research Letters*, vol. 37, doi:10.1029/2010GL045440.  
757  
758 Jackson, J.M., Carmack, E.C., McLaughlin, F.A., Allen, S.E., and Ingram, R.G. (2010)  
759 Identification, characterization, and change of near-surface temperature maximum in the Canada  
760 Basin, 1993-2008. *Journal Geophysical Research*, vol. 115, doi:10.1029/2009JC005265.  
761  
762 Jain, S., Lall, U., and Mann, M.E. (1999) Seasonality and interannual variations of Northern  
763 Hemisphere temperature: Equator-to-pole gradient and ocean-land contrast. *Journal of Climate*,  
764 vol. 12, 1086-1100.  
765  
766 Jiang, H., Eiriksson, J., Schulz, M., Knudsen, K.-L., and Seidenkrantz, M.-S. (2005) Evidence  
767 for solar forcing of sea-surface temperature on the North Icelandic Shelf during the late  
768 Holocene. *Geology*, vol. 33, 73-76.  
769  
770 Judge, P.G., Lockwood, G.W., Radick, R.R., Henry, G.W., Shapiro, A.I., Schmutz, W., and  
771 Lindsey, C. (2012) Confronting a solar irradiance reconstruction with solar and stellar data.  
772 *Astronomy and Astrophysics*, vol. 544, A88, doi:10.1051/0004-6361/201218903.  
773  
774 Kamenos, N.A. (2010) North Atlantic summers have warmed more than winters since 1353, and  
775 the response of marine zooplankton. *Proceedings of the (U.S.) National Academy of Sciences*,  
776 vol. 107, 22442-22447.  
777  
778 Karamperidou, C., Cioffi, F., and Lall, U. (2012) Surface temperature gradients as diagnostic  
779 indicators of mid-latitude circulation dynamics. *Journal of Climate*, vol. 25, 4154-4171.  
780  
781 Kendall, M.G. (1938) A new measure of rank correlation. *Biometrika*, vol. 30, 81-93.  
782

783 Kleint, L., Berdyugina, S.V., Shapiro, A.I., and Bianda, M. (2010) Solar turbulent magnetic  
784 fields: Surprisingly homogeneous distribution during the solar minimum. *Astronomy and*  
785 *Astrophysics*, vol. 524, A37.  
786  
787 Kopp, G., and Lean, J.L. (2011) A new, lower value of total solar irradiance: Evidence and  
788 climate significance. *Geophysical Research Letters*, vol. 38, doi:10.1029/2010GL045777.  
789  
790 Kroeger, K.F., and Funnell, R.H. (2012) Warm Eocene climate enhanced petroleum generation  
791 from Cretaceous source rock: A potential climate feedback mechanism? *Geophysical Research*  
792 *Letters*, vol. 39, doi:10.1029/2011GL050345.  
793  
794 Kukla, G., and Gavin, J. (2004) Milankovitch climate reinforcements. *Global and Planetary*  
795 *Change*, vol. 40, 27-48.  
796  
797 Kukla, G., and Gavin, J. (2005) Did glacials start with global warming? *Quaternary Science*  
798 *Reviews*, vol. 24, 1547-1557.  
799  
800 Langen, P.L., and Alexeev, V.A. (2007) Polar amplification as a preferred response in an  
801 idealized aquaplanet GCM. *Climate Dynamics*, vol. 29, 305-317.  
802  
803 Laskar, J., Fienga, A., Gastineau, M., and Manche, H. (2011) La2010: A new orbital solution for  
804 the long-term motion of the Earth. *Astronomy and Astrophysics*, vol. 532, A89.  
805  
806 Laskar, J., Joutel, F., and Boudin, F. (1993) Orbital, precessional, and insolation quantities for  
807 the Earth from -20Myr to +10Myr. *Astronomy and Astrophysics*, vol. 270, 522-533.  
808  
809 Latif, M., Boning, C., Willebrand, J., Biastoch, A., Dengg, J., Keenlyside, N., Schweckendiek,  
810 U., and Madec, G. (2006) Is the thermohaline circulation changing? *Journal of Climate*, vol. 19,  
811 4631-4637.  
812  
813 Latif, M., Roeckner, E., Esch, M., Haak, H., Hagemann, S., Jungclaus, J., Legutke, S., Marsland,  
814 S., Mikolajewicz, U., and Mitchell, J. (2004) Reconstructing, monitoring, and predicting  
815 multidecadal-scale changes in the North Atlantic thermohaline circulation with sea surface  
816 temperature. *Journal of Climate*, vol. 17, 1605-1614.  
817  
818 Laurmann, J.A., and W.L. Gates (1977) Statistical considerations in the evaluation of climatic  
819 experiments with atmospheric general circulation models. *Journal of the Atmospheric Sciences*,  
820 vol. 34, 1187-1199.  
821  
822 Lee, S., Felstein, S., Pollard, D., and White, T. (2011) Do planetary wave dynamics contribute to  
823 equable climates? *Journal of Climate*, vol. 24, 2391-2404.  
824  
825 Lindzen, R.S. (1994) Climate dynamics and global change. *Annual Review of Fluid Mechanics*,  
826 vol. 26, 353-378.  
827

828 Lindzen, R.S. (2012) Climate physics, feedbacks, and reductionism (and when does reductionism  
829 go too far?). *European Physical Journal Plus*, vol. 127, doi:10.1140/epjp/i2012-12052-8.  
830

831 Lindzen, R.S., and Pan, W. (1994) A note on orbital control of equator-to-pole heat fluxes.  
832 *Climate Dynamics*, vol. 10, 49-57.  
833

834 Liu, J., Song, M., Hu, Y., and Ren, X. (2012) Changes in the strength and width of the Hadley  
835 circulation since 1871. *Climate of the Past*, vol. 8, 1169-1175.  
836

837 Liu, Z., Cleaveland, L.C., and Herbert, T.D. (2008) Early onset and origin of 100-kyr cycles in  
838 Pleistocene tropical SST records. *Earth and Planetary Science Letters*, vol. 265, 703-715.  
839

840 Lockwood, G.W., Skiff, B.A., Henry, G.W., Henry, S., Radick, R.R., Baliunas, S.L., Donahue,  
841 R.A., and Soon, W. (2007) Patterns of photometric and chromospheric variation among sun-like  
842 stars: A 20 year perspective. *The Astrophysical Journal Supplement Series*, vol. 171, 260–303.  
843

844 Lund, D.C., Lynch-Stieglitz, J., and Curry, W.B. (2006) Gulf Stream density structure and  
845 transport during the past millennium. *Nature*, vol. 444, 601-604.  
846

847 McKittrick, R.R., and Michaels, P.J. (2007) Quantifying the influence of anthropogenic surface  
848 processes and inhomogeneities on gridded global climate data. *Journal Geophysical Research*,  
849 vol. 112, doi:10.1029/2007JD008465.  
850

851 McKittrick, R., and Tole, L. (2012) Evaluating explanatory models of the spatial pattern of  
852 surface climate trends using model selection and Bayesian averaging methods, *Climate*  
853 *Dynamics*, in press, doi:10.1007/s00382-012-1418-9.  
854

855 Mörner, N.-A. (2010) Solar minima, Earth’s rotation and Little Ice Ages in the past and in the  
856 future: The North Atlantic-European case. *Global and Planetary Change*, vol. 72, 282-293.  
857

858 Murakami, S., Ohgaito, R., Abe-Ouchi, A., Crucifix, M., and Otto-Bliesner, B.L. (2008) Global-  
859 scale energy and freshwater balance in glacial climate: A comparison of three PMIP2 LGM  
860 simulation. *Journal of Climate*, vol. 21, 5008-5033.  
861

862 Orozco Suarez, D., and 12 co-authors (2007) Quiet-sun internetwork magnetic fields from the  
863 inversion of *Hinode* measurements. *The Astrophysical Journal Letters*, vol. 670, L61–L64.  
864

865 Orozco Suarez, D., and Rubio, L.R.B. (2012) Analysis of quiet sun internetwork magnetic fields  
866 based on linear polarization signals. *The Astrophysical Journal*, vol. 751: 2, doi:10.1088/0004-  
867 637X/751/1/2.  
868

869 Orvik, K.A., and Skagseth, O. (2005) Heat flux variations in the eastern Norwegian Atlantic  
870 Current toward the Arctic from moored instruments, 1995-2005. *Geophysical Research Letters*,  
871 vol. 32, doi:10.1029/2005GL023487.  
872

873 Pierrehumbert, R.T. (2002) The hydrologic cycle in deep-time climate problems. *Nature*, vol.  
874 419, 191-198.  
875  
876 Polyakov, I.V. and 22 co-authors. (2005) One more step toward a warmer Arctic. *Geophysical*  
877 *Research Letters*, vol. 32, doi:10.1029/2005GL023740.  
878  
879 Polyakov, I.V., Alexeev, V.A., Bhatt, U.S., Polyakova, E.I., and Zhang, X. (2010a) North  
880 Atlantic warming: Patterns of long-term trend and multidecadal variability. *Climate Dynamics*,  
881 vol. 34, 439-457.  
882  
883 Polyakov, I.V. and 17 co-authors. (2010b) Arctic ocean warming contributes to reduced polar ice  
884 cap. *Journal of Climate*, vol. 40, 2743-2756.  
885  
886 Pross, J. and 17 co-authors. (2012) Persistent near-tropical warmth on the Antarctic continent  
887 during the early Eocene epoch. *Nature*, vol. 488, 73-77.  
888  
889 Raymo, M.E., and Nisancioglu, K. (2003) The 41 kyr world: Milankovitch's other unsolved  
890 mystery. *Paleoceanography*, vol. 18, doi:10.1029/2002PA000791.  
891  
892 Rayner, N.A., Brohan, P., Parker, D.E., Folland, C.K., Kennedy, J.J., Vanicek, M., Ansell, T.,  
893 and Tett, S.F.B. (2006) Improved analyses of changes and uncertainties in marine temperature  
894 measured in situ since the mid-nineteenth century: the HadSST2 dataset. *Journal Climate*, vol.  
895 19, 446-469.  
896  
897 Reverdin, G. (2010) North Atlantic subpolar gyre surface variability (1895-2009). *Journal of*  
898 *Climate*, vol. 23, 4571-4584.  
899  
900 Rind, D. (1998) Latitudinal temperature gradients and climate change. *Journal of Geophysical*  
901 *Research*, vol. 103, 5943-5971.  
902  
903 Robson, J., Sutton, R., Lohmann, K., Smith, D., and Palmer, D. (2012) Causes of the rapid  
904 warming of the North Atlantic Ocean in the mid 1990s. *Journal of Climate*, vol. 25, 4116-4134.  
905  
906 Rose, B.E., and Ferreira, D. (2012) Ocean heat transport and water vapor greenhouse in a warm  
907 equable climate: A new look at the low gradient paradox. *Journal of Climate*, in press,  
908 doi:10.1175/JCLI-D-11-0547.1.  
909  
910 Sarafanov, A., Falina, A., Sokov, A., and Demidov, A. (2008) Intense warming and salinification  
911 of intermediate waters of southern origin in the eastern subpolar North Atlantic in the 1990s to  
912 mid-2000s. *Journal Geophysical Research*, vol. 113, doi:10.1029/2008JC004975.  
913  
914 Scafetta, N., and Willson, R. (2009) ACRIM-gap and TSI trend issue resolved using a surface  
915 magnetic flux TSI proxy model. *Geophysical Research Letters*, vol. 36,  
916 doi:10.1029/2008GL036307.  
917

918 Schmidt, G.A., and 15 co-authors (2011) Climate forcing reconstructions for use in PMIP  
919 simulations of the last millennium (v1.0). *Geoscientific Model Development*, vol. 4, 33–45.  
920

921 Schnerr, R.S., and Spruit, H.C. (2011) The brightness of magnetic field concentrations in the  
922 quiet Sun. *Astronomy and Astrophysics*, vol. 532, A136, doi:10.1051/0004-6361/201015976.  
923

924 Schuhle, U., Wilhelm, K., Hollandt, J., Lemaire, P., and Pauluhn, A. (2000) Radiance variations  
925 of the quiet Sun at far-ultraviolet wavelengths. *Astronomy and Astrophysics*, vol. 354, L71-L74.  
926

927 Screen, J.A., and Simmonds, I. (2010) The central role of diminishing sea ice in recent Arctic  
928 temperature amplification. *Nature*, vol. 464, 1334-1337.  
929

930 Screen, J.A., and Simmonds, I. (2011) Erroneous Arctic temperature trends in the ERA-40  
931 Reanalysis: A closer look. *Journal of Climate*, vol. 24, 2620-2627.  
932

933 Semmler, T., Jacob, D., Heinke Schlunzen, K., and Podzin, R. (2005) The water and energy  
934 budget of the Arctic atmosphere. *Journal of Climate*, vol. 18, 2515-2530.  
935

936 Shaffrey, L., and Sutton, R. (2006) Bjerknes compensation and the decadal variability of the  
937 energy transports in a coupled climate model. *Journal of Climate*, vol. 19, 1167-1181.  
938

939 Shapiro, A.I., Schmutz, W., Rozanov, E., Schoell, M., Haberreiter, M. Shapiro, A.V., and Nyeki,  
940 S. (2011) A new approach to the long-term reconstruction of the solar irradiance leads to a large  
941 historical solar forcing. *Astronomy and Astrophysics*, vol. 529, A67.  
942

943 Shimada, K., Kamoshida, T., Itoh, M., Nishino, S., Carmack, E., McLaughlin, F., Zimmermann,  
944 S., and Proshuntinsky, A. (2006) Pacific Ocean inflow: Influence on catastrophic reduction of  
945 sea ice cover in the Arctic Ocean. *Geophysical Research Letters*, vol. 33,  
946 doi:10.1029/2005GL025624.  
947

948 Sluijs, A., and 15 co-authors (2006) Subtropical Arctic Ocean temperatures during the  
949 Palaeocene/Eocene thermal maximum. *Nature*, vol. 441, 610-613.  
950

951 Smedsrud, L.H., Sorteberg, A., and Kloster, K. (2008) Recent and future changes of the Arctic  
952 sea-ice cover. *Geophysical Research Letters*, vol. 35, doi:10.1029/2008GL034813.  
953

954 Soon, W. W.-H. (2005) Variable solar irradiance as a plausible agent for multidecadal variations  
955 in the Arctic-wide surface air temperature record of the past 130 years. *Geophysical Research  
956 Letters*, vol. 32, doi:10.1029/2005GL023429.  
957

958 Soon, W. (2009) Solar Arctic-mediated climate variation on multidecadal to centennial  
959 timescales: Empirical evidence, mechanistic explanation, and testable consequences. *Physical  
960 Geography*, vol. 30, 144–184.  
961

962 Soon, W., Dutta, K., Legates, D.R., Velasco, V., and Zhang, W. (2011) Variation in surface air  
963 temperature of China during the 20<sup>th</sup> Century. *Journal of Atmospheric and Solar-Terrestrial*  
964 *Physics*, vol. 73, 2331-2344.

965  
966 Spearman, C. (1904) The proof and measurement of association between two things. *The*  
967 *American Journal of Psychology*, vol. 15, 72-101.

968  
969 Stenflo, J.O. (2012) Scaling laws for magnetic fields on the quiet Sun. *Astronomy and*  
970 *Astrophysics*, vol. 541, A17, doi:10.1051/0004-6361/201218939.

971  
972 Stenflo, J.O., and Kosovichev, A.G. (2012) Bipolar magnetic regions on the Sun: Global analysis  
973 of the *SOHO*/MDI data set. *The Astrophysical Journal*, vol. 745: 129, doi:10.1088/0004-  
974 637X/745/129.

975  
976 Stone, P.H. (1978) Constraints on dynamical transports of energy on a spherical planet.  
977 *Dynamics of Atmospheres and Oceans*, vol. 2, 123-139.

978  
979 Thiebaux, H.J., and F.W. Zwiers (1984) The interpretation and estimation of effective sample  
980 size. *Journal of Climate and Applied Meteorology*, vol. 23, 800-811.

981  
982 Toole, J.M., Timmermanns, M.-L., Perovich, D.K., Krishfield, R.A., Proshutinsky, A., and  
983 Richter-Menge, J.A. (2010) Influences of the ocean surface mixed layer and thermohaline  
984 stratification on Arctic sea ice in the central Canada Basin. *Journal Geophysical Research*, vol.  
985 115, doi:10.1029/2009JC005660.

986  
987 Trenberth, K.E., and Caron, J.M. (2001) Estimates of meridional atmosphere and ocean heat  
988 transport. *Journal of Climate*, vol. 14, 3433-3443.

989  
990 Trujillo Bueno, J., Shchukina, N., Asensio Ramos, A. (2004) A substantial amount of hidden  
991 magnetic energy in the quiet Sun. *Nature*, vol. 430, 326-329.

992  
993 Tyndall, J. (1872) *The Forms of Water in Clouds and Rivers Ice and Glaciers* (International  
994 Science Library, The Werner Company, Akron OH, 196 pp).

995  
996 Vallis, G.K., and Farneti, R. (2009) Meridional energy transport in the coupled atmosphere-  
997 ocean system: Scaling and numerical experiments *Quarterly Journal of the Royal*  
998 *Meteorological Society*, vol. 135, 1643-1660.

999  
1000 van Loon, H., Brown, J., and Milliff, R.F. (2012) Trends in sunspots and North Atlantic sea-level  
1001 pressure. *Journal Geophysical Research*, vol. 117, doi:10.1029/2012JD017502.

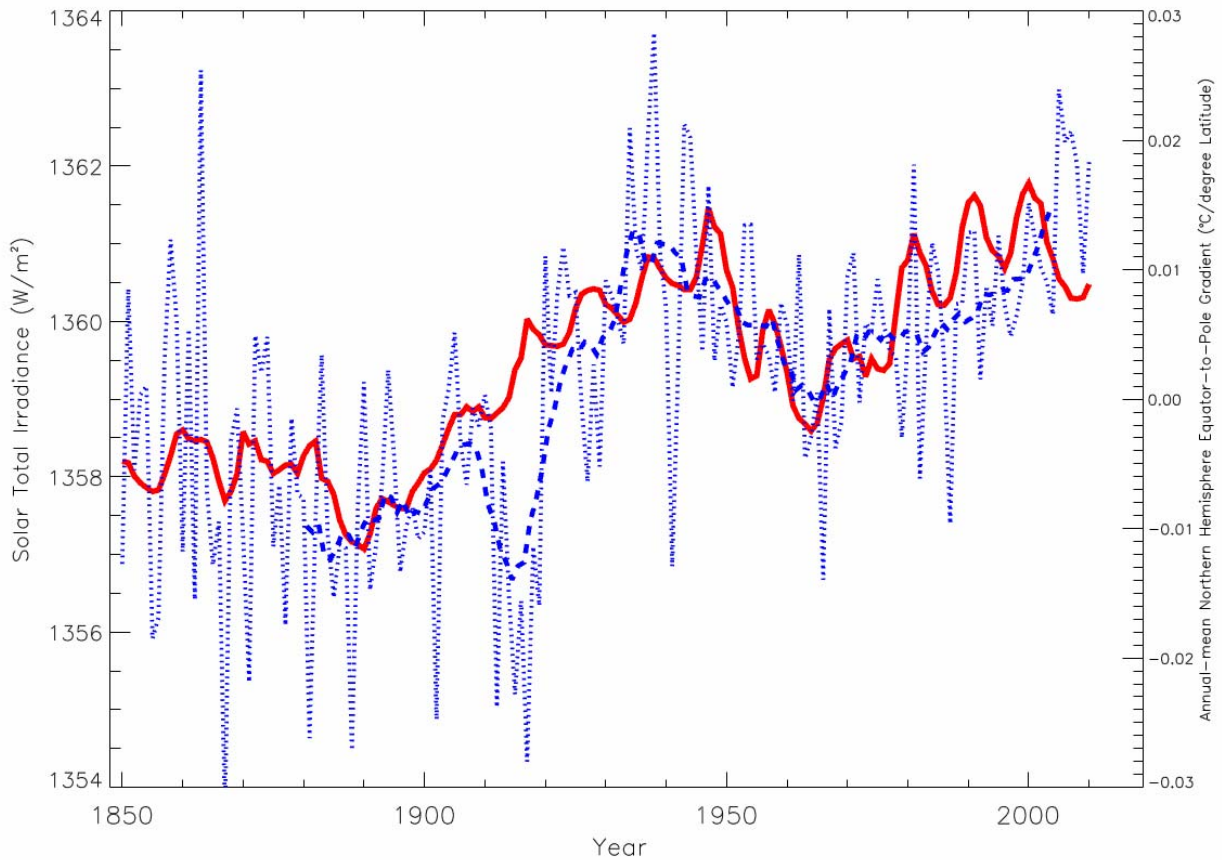
1002  
1003 van Loon, H., and Meehl, G.A. (2012) The Indian summer monsoon during peaks in the 11 year  
1004 sunspot cycle. *Geophysical Research Letters*, vol. 39, doi:10.1029/2012JD051977.

1005  
1006 Weng, H. (2005) The influence of the 11 yr solar cycle on the interannual-centennial climate  
1007 variability. *Journal of Atmospheric and Solar-Terrestrial Physics*, vol. 67, 793-805.

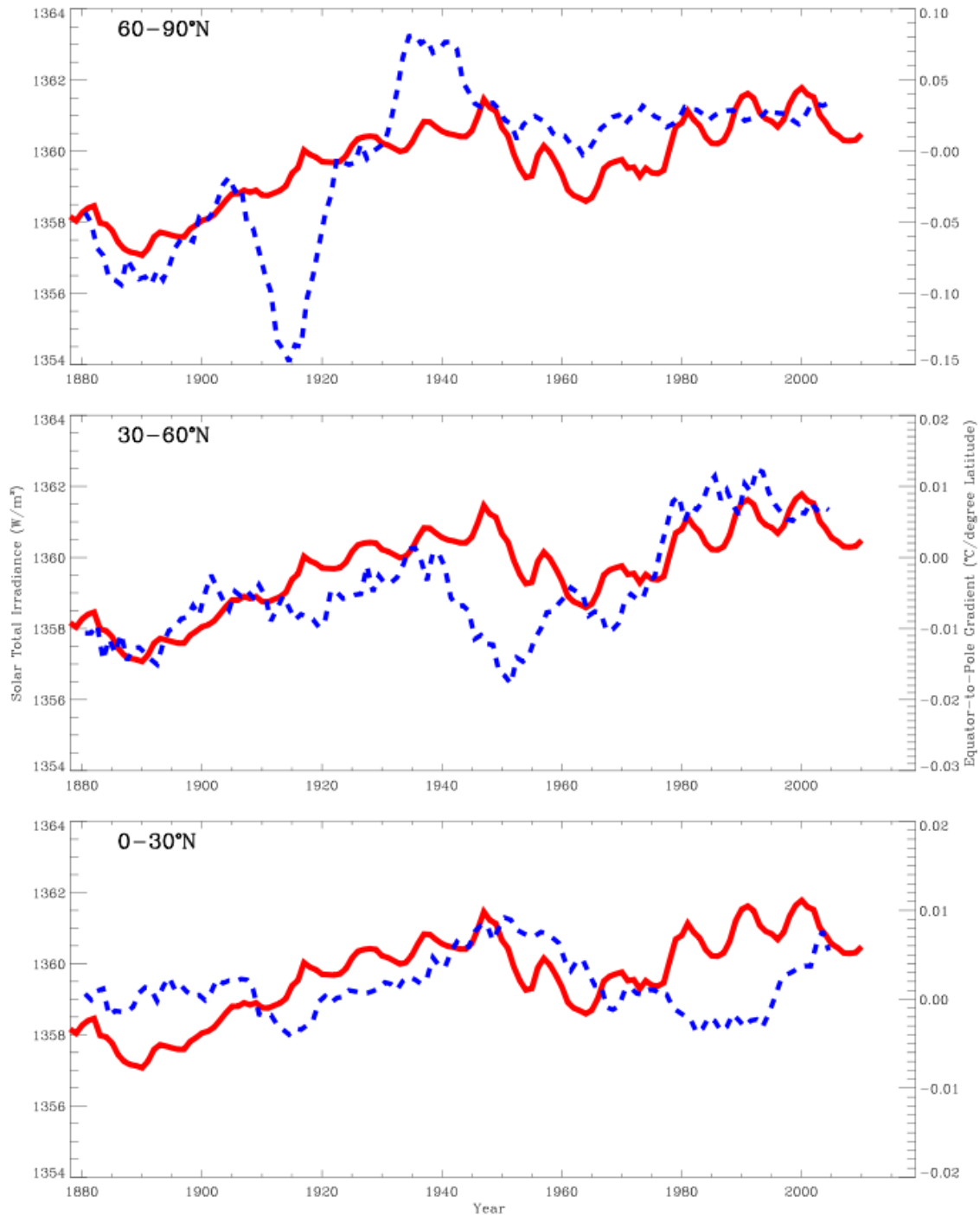
1008  
1009 Weng, H. (2012a) Impact of multi-scale solar activity on climate. Part I: Atmospheric circulation  
1010 patterns and climate extremes. *Advances in Atmospheric Sciences*, vol. 29, 867-886.  
1011  
1012 Weng, H. (2012b) Impact of multi-scale solar activity on climate. Part II: Dominant timescales in  
1013 decadal-centennial climate variability. *Advances in Atmospheric Sciences*, vol. 29, 887-908.  
1014  
1015 Willis, J.K. (2010) Can in situ floats and satellite altimeters detect long-term changes in Atlantic  
1016 Ocean overturning? *Geophysical Research Letters*, vol. 37, doi:10.1029/2010GL042372.  
1017  
1018 Willson, R. C. (2011) Revision of ACRIMSAT/ACRIM3 TSI results based on LASP/TRF  
1019 diagnostic test results for the effects of scattering, diffraction and basic SI scale traceability.  
1020 Abstract for 2011 Fall AGU meeting (session GC21).  
1021  
1022 Woodgate, R.A., Weingartner, T., and Lindsay, R. (2010) The 2007 Bering Strait oceanic heat  
1023 flux and anomalous Arctic sea-ice. *Geophysical Research Letters*, vol. 37,  
1024 doi:10.1029/2009GL041621.  
1025  
1026 Wu, Y., Ting, M., Seager, R., Huang, H.-P., and Cane, M.A. (2011) Changes in storm tracks and  
1027 energy transports in a warmer climate simulated by the GFDL CM2.1 model *Climate Dynamics*,  
1028 vol. 37, 53-72.  
1029  
1030 Wunsch, C. (2005) The total meridional heat flux and its oceanic and atmospheric partition.  
1031 *Journal of Climate*, vol. 18, 4374-4380.  
1032  
1033 Wunsch, C. (2010) Towards understanding the Paleocean. *Quaternary Science Reviews*, vol. 29,  
1034 1960-1967.  
1035  
1036 Yang, X.-Y., Fyfe, J.C., and Flato, G.M. (2010) The role of poleward energy transport in Arctic  
1037 temperature evolution. *Geophysical Research Letters*, vol. 37, doi:10.1029/2010GL043934.  
1038  
1039 Yue, S., P. Pilon, and G.S. Cavadias (2002) Power of the Mann-Kendall and Spearman's rho  
1040 tests for detecting monotonic trends in hydrological series. *Journal of Hydrology*, vol. 259, 254-  
1041 271.  
1042  
1043 Zelinka, M.D., and Hartmann, D.L. (2012) Climate feedbacks and their implications for  
1044 poleward energy flux changes in a warming climate. *Journal of Climate*, vol. 25, 608-624.  
1045  
1046 Zhang, Q., Soon, W.H., Baliunas, S.L., Lockwood, G.W., Skiff, B.A., and Radick, R.R. (1994) A  
1047 method of determining possible brightness variations of the Sun in past centuries from  
1048 observations of solar-type stars. *The Astrophysical Journal Letters*, vol. 427, L111-L114.  
1049  
1050 Zhang, X., Sorteberg, A., Zhang, J., Gerdes, R., and Comiso, J.C. (2008) Recent radical shifts of  
1051 atmospheric circulations and rapid changes in Arctic climate system. *Geophysical Research*  
1052 *Letters*, vol. 35, doi:10.1029/2008GL035607.

1053 **Table 1:** Square of the Pearson Product-Moment Correlation Coefficient (*i.e.*, the Coefficient of  
 1054 Determination) and Kendall’s Tau non-parametric correlation coefficient between total solar  
 1055 irradiance (TSI) and Northern Hemispheric EPTGs (smoothed by a 10-year running mean) from  
 1056 1880 to 2010 (1850 to 1879 was discarded for analysis due to a lack of data reliability). Values  
 1057 that are statistically significant at a Type I error level of 0.05 using an ‘effective degrees of  
 1058 freedom’ of 10 are denoted by an asterisk (see text).  
 1059

	Coefficient of Determination				Kendall’s Tau			
	0°-30°	30°-60°	60°-90°	0°-90°	0°-30°	30°-60°	60°-90°	0°-90°
<b>Annual-mean</b>	0.04	0.37	<b>0.50*</b>	<b>0.70*</b>	0.11	0.42	<b>0.53*</b>	<b>0.63*</b>
<b>Winter</b>	0.34	0.22	<b>0.48*</b>	<b>0.57*</b>	0.36	0.24	0.42	<b>0.54*</b>
<b>Spring</b>	0.17	0.45	0.16	<b>0.62*</b>	0.23	<b>0.47*</b>	0.30	<b>0.58*</b>
<b>Summer</b>	0.27	0.01	0.42	<b>0.60*</b>	-0.31	0.03	0.38	<b>0.51*</b>
<b>Autumn</b>	0.00	0.12	0.36	<b>0.50*</b>	0.02	0.24	<b>0.52*</b>	<b>0.53*</b>

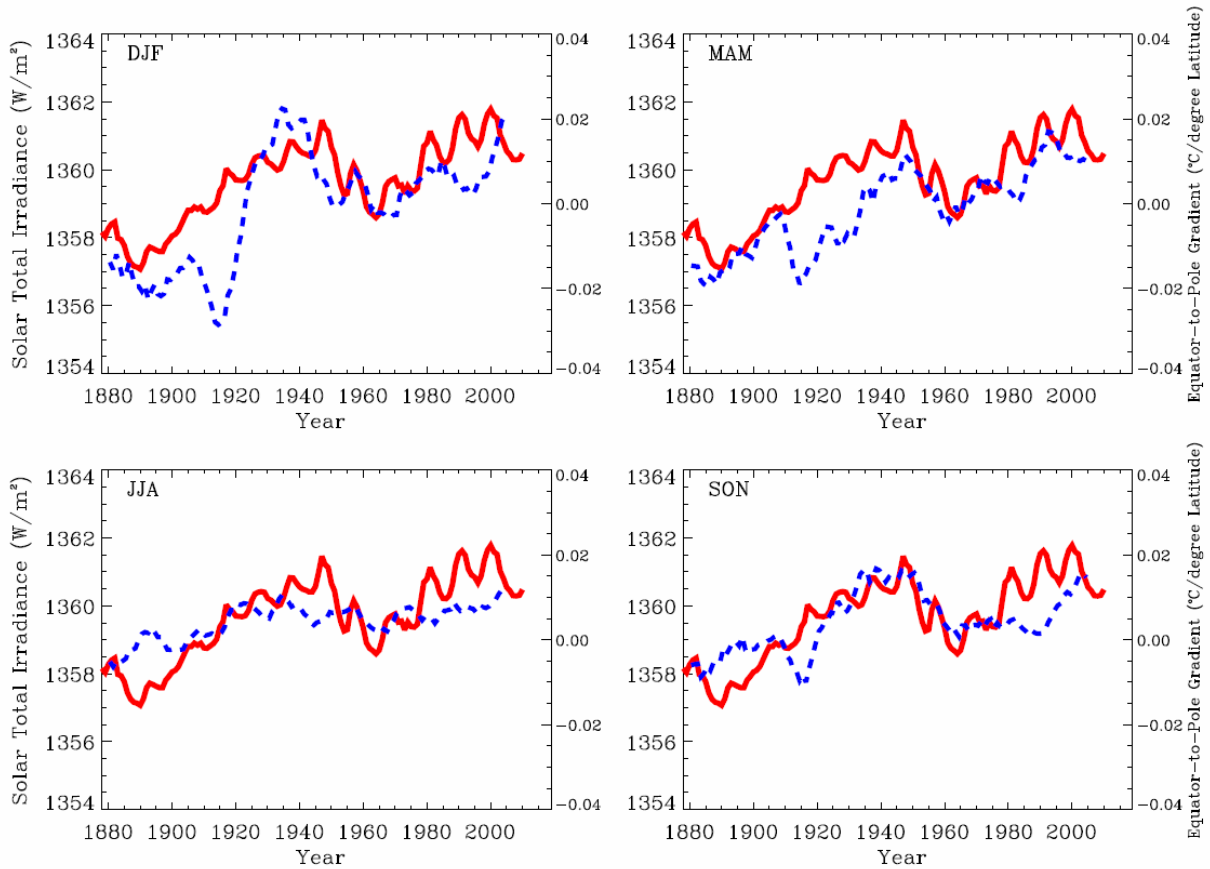


1060  
 1061 **Figure 1:** Annual-mean EPTG over the entire Northern Hemisphere ( $^{\circ}\text{C}/\text{degree latitude}$ ; dotted  
 1062 blue line) and smoothed 10-year running mean (dashed blue line) versus the estimated total  
 1063 solar irradiance TSI ( $\text{Wm}^{-2}$ ; solid red line) of Hoyt and Schatten (1993; with updates by N.  
 1064 Scafetta) from 1850 to 2010. We emphasize the relationship especially on multi-decadal  
 1065 timescales and report the TSI correlations only with the smoothed EPTG series with 10-year  
 1066 running means (since 1880) in Table 1. Increased TSI is related to decreased temperature  
 1067 gradients between the Equator and the Arctic (*i.e.*, more positive EPTG values) and vice  
 1068 versa.



1069  
 1070  
 1071  
 1072  
 1073  
 1074  
 1075  
 1076  
 1077

**Figure 2:** Northern Hemisphere EPTGs for the three latitude bands: 0° to 30°N, 30°N to 60°N, and 60°N to 90°N, smoothed by 10-year running means (°C/degree latitude; dotted blue curves) versus the estimated total solar irradiance TSI ( $\text{Wm}^{-2}$ ; solid red curves) of Hoyt and Schatten (1993; with updates by N. Scafetta) from 1880 to 2010. Increased TSI is related to decreased temperature gradients between the Equator and the Arctic (*i.e.*, more positive EPTG values) and vice versa. Owing to the large dynamic range of the surface temperature gradients across the latitudinal bands, the vertical scales in the three latitudinal bands are different in each panel.



1078  
 1079 **Figure 3:** Northern Hemisphere EPTGs for four seasons (DJF, MAM, JJA and SON) smoothed  
 1080 by 10-year running means ( $^{\circ}\text{C}/\text{degree latitude}$ ; dotted blue curves) versus the estimated total  
 1081 solar irradiance TSI ( $\text{Wm}^{-2}$ ; solid red curves) of Hoyt and Schatten (1993; with updates by  
 1082 N. Scafetta) from 1880 to 2010. Increased TSI is related to decreased temperature gradients  
 1083 between the Equator and the Arctic (*i.e.*, more positive EPTG values) and vice versa.